JOURNAL OF SPACECRAFT AND ROCKETS
Vol. 34, No. 5, September–October 1997

Enthalpy Effects on Hypervelocity Boundary-Layer Transition: Ground Test and Flight Data

Philippe H. Adam* and Hans G. Hornung†
California Institute of Technology, Pasadena, California 91125

Boundary-layer-transition experiments on a 5-deg half-angle cone at 0-deg angle of attack were performed in the T5 hypervelocity shock tunnel. The test gases investigated included air, nitrogen, and carbon dioxide. Reservoir enthalpies were varied from 3 to 27 MJ/kg and reservoir pressures from 10 to 95 MPa, depending on the gas and tunnel settings. No clear relationship is found to exist between the transition Reynolds number based on the boundary-layer-edge conditions and the reservoir enthalpy. However, when the reference temperature conditions are used instead, the different test gases are distinguishable and ordered according to their dissociation energy. Data from a free-flight experiment are also compared with the shock tunnel experiments. When the transition Reynolds numbers are evaluated at the boundary-layer-edge conditions, they are an order of magnitude higher than the tunnel results. However, when the reference conditions are used, the flight data fall within the same range as the experiments, although the trend with reservoir enthalpy is reversed.

Nomenclature

h = enthalpy, MJ/kg
M = Mach number
P = pressure, Pa
$\dot{q}$ = heat transfer rate, MW/m^2
Re = Reynolds number
r = recovery factor
St = Stanton number
T = temperature, K
u = velocity, m/s
x = axial distance, m
μ = viscosity, kg/m-s
ρ = density, kg/m^3

Subscripts

a = adiabatic
e = boundary-layer edge
tr = transition
w = wall
0 = reservoir
∞ = freestream

Superscript

$*$ = reference condition

Introduction

SIMULATING atmospheric re-entry in the laboratory is best achieved when a few essential parameters are reproduced. Obviously, the fluid must be the same: for example, air in the case of Earth or carbon dioxide in the case of Mars. Most importantly, however, the flight speed must be matched to bring out the proper physical and chemical processes that characterize re-entry flows on the order of several kilometers per second. These flows are commonly referred to as hypervelocity and, along with the high speeds, one usually refers to the correspondingly high enthalpy.

With these parameters in mind, the T5 free-piston hypervelocity shock tunnel was designed and built at the Graduate Aeronautical Laboratories at the California Institute of Technology (GALCIT).[1] With air and nitrogen as test gases, T5 is capable of producing specific reservoir enthalpies from $h_0 = 4$ to 27 MJ/kg at stagnation pressures from $P_0 = 20$ to over 100 MPa. In the Mach 5 freestream, after the fluid is accelerated through a nozzle, the unit Reynolds number achieved within the performance envelope then varies from around 1×10^6 to close to 10×10^6 m^{-1}. This range makes the facility particularly well suited to the study of hypervelocity boundary layers and, in particular, enthalpy effects on the flow. For this reason, one of the very first projects undertaken in the tunnel was the investigation of boundary-layer transition, a subject extensively studied in cold tunnels but still poorly understood and on which very little is known at high enthalpies. Feasibility and preliminary results of boundary-layer experiments on a sharp cone were described by Germain et al.[2] and, more recently, by Germain and Hornung.[3]

One result that stood out from these transition experiments was that there was no discernible trend between the transition Reynolds number Re_{tr} based on the boundary-layer-edge conditions and the specific reservoir enthalpy h_0. However, when evaluated at the reference conditions, which better represent the overall inner state of the boundary layer, the reference transition Reynolds number Re^*_{tr} did appear to correlate with h_0. In fact, over the enthalpy range considered, values of Re^*_{tr} increased exponentially with respect to h_0, with the data for air falling consistently above those for nitrogen. This result is shown in Fig. 1 along with older data from cold tunnels[4,5] (also see Ref. 6). The open symbols for the air and nitrogen data correspond to runs where the flow was almost fully laminar with a hint of transition. The stabilizing effect of enthalpy was attributed to the fact that, for a given enthalpy, the gas with the lower dissociation energy might tend to yield higher Re_{tr} (Ref. 3).

In this paper, some light will be shed on the influence of dissociation energy on the Re_{tr}. To complement the existing experimental results cited, additional data in air are obtained on a more densely instrumented model, thereby reducing some of the uncertainty in the measured transition locations. More importantly, however, Re_{tr} are measured for a wide range of enthalpies in carbon dioxide flows. Dissociation effects appear at lower enthalpy in carbon dioxide than in air or nitrogen, and it is expected that differences between carbon dioxide and the other gases will be more pronounced than those between air and nitrogen.

Another issue of interest is the relation of these results obtained in the laboratory to actual free-flight re-entry data. It is generally accepted that care must be taken when comparing transition data obtained in different tunnels because transition mechanisms depend on the disturbance environments, which can be quite different in different facilities.[7] Best agreement with free-flight results is obtained

Received Dec. 20, 1996; revision received June 6, 1997; accepted for publication June 13, 1997.

*Graduate Research Assistant, Graduate Aeronautical Laboratories. Student Member AIAA.

†Director, Graduate Aeronautical Laboratories, and Kelly Johnson Professor of Aeronautics. Member AIAA.

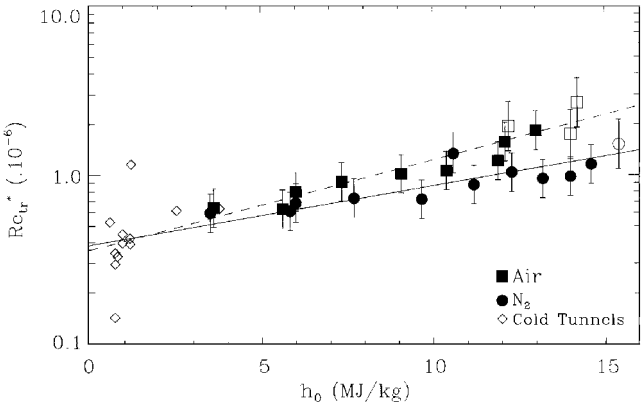

Fig. 1 Re_{tr} **evaluated at reference conditions.**[3,6]

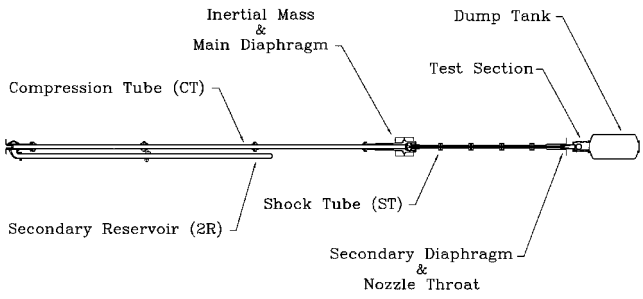

Fig. 2 T5 hypervelocity shock tunnel.

with figures from quiet tunnels, conventional tunnels usually giving Re_{tr} up to an order of magnitude too low.[8] In this paper, some flight data are compared with results from T5. Although the flight data were obtained over a very limited enthalpy range,[9] this range is nevertheless within the performance envelope of the shock tunnel. Furthermore, the detailed flight characteristics and transition information make it possible to directly compare these flight data with the laboratory data.

T5 Free-Piston Hypervelocity Shock Tunnel

All experiments were carried out in the T5 hypervelocity shock tunnel (Fig. 2) at GALCIT. The facility operates in the standard reflected shock tunnel mode with the exception that the high pressure and temperature on the driver side are produced by free-piston adiabatic compression.

The piston is launched by high-pressure air from a secondary air reservoir, compressing the driver gas, a mixture of helium and argon, to the desired diaphragm burst pressure. Typical secondary reservoir pressures vary from 5 to 13 MPa and burst pressures from 30 to 120 MPa. Once the diaphragm bursts, a shock wave travels at speeds from 2 to 5 km/s through the shock tube part of the tunnel, compressing and heating the test gas. When the shock wave reflects off the end of the tube, a high-pressure, high-temperature reservoir is produced. For air and nitrogen runs, reservoir pressures vary from 10 to 85 MPa and enthalpies from 4 to 27 MJ/kg. For carbon dioxide runs, reservoir pressures vary from 40 to 95 MPa and enthalpies from 3 to 10 MJ/kg.

The reservoir gas is then accelerated through a contoured nozzle into the test section. The useful test time is approximately 1 ms but varies with reservoir enthalpy. A study of the flow establishment and driver gas contamination in T5 can be found in Ref. 10. The nozzle is designed to produce a freestream around Mach 5 with air. Freestream unit Reynolds numbers vary from 2×10^6 to 10×10^6 m^{-1} in air and nitrogen and from 4×10^6 to 20×10^6 m^{-1} in carbon dioxide.

Pressure transducers at various locations inside the shock tube give the shock speed v_s ($\pm 2\%$), initial shock tube pressure P_1 ($\pm 1\%$), and stagnation pressure P_0 ($\pm 5\%$). From these numbers, an equilibrium calculation gives the remaining reservoir conditions such as composition and enthalpy. A quasi-one-dimensional nonequilibrium nozzle calculation is then performed to find the freestream conditions. Uncertainties in the calculated compositions do affect the freestream gasdynamic properties, but the resulting errors, in the temperature T_∞, for example, are typically no more than 5%. Further details on the performance and operation of the T5 shock tunnel can be found in Ref. 11.

Model and Instrumentation

The model used for these experiments is a 1-m-long, 5-deg half-angle sharp cone (Fig. 3) divided into three sections. The main body of the model is 790 mm long and made of aluminum. It is split into two dove-tailed halves that are secured by sliding over each other. Only the bottom half is instrumented; the top half is left free for future experiments. An intermediate 127-mm-long section screws into the main body; it is also made of aluminum. Into this last piece fits a 76-mm tip made of molybdenum. New tips have a nose radius on the order of 0.001 in. and can be replaced when excessive blunting occurs or when other damage due to the intense heating becomes significant. Typically, the nose radius stabilizes around 0.005 in. after several shots, but no noticeable effect has been observed on the measurements farther back on the model.[3,12]

The cone is mounted inside the test section on a sting at 0-deg angle of attack and protrudes slightly into the nozzle to be continuously submerged in a uniform freestream during a run. It was originally instrumented with 15 fast-response coaxial thermocouples of type E (chromel-constantan). For this series of tests, that number was increased to 53, thereby decreasing the uncertainty in the transition location. Because the data acquisition is only equipped to record 48 traces at a time, 5 thermocouples act as spares and can be quickly connected in between runs should any of the activated gauges fail or should better resolution be desired on different regions of the model.

All thermocouples are mounted flush with the model surface. The signal during the test is first amplified by a factor of 500, then sampled at 200 kHz. During these tests some traces were also recorded at 1 and 5 MHz. The voltage is converted to temperature with a standard correlation for chromel-constantan thermocouples. Heat flux is then obtained following an indirect one-dimensional, semi-infinite slab theory.[13] Accuracy is on the order of 10–15% at low enthalpies and around 20% at high enthalpies. Nevertheless, repeatability of tests is very good and shot-to-shot variations are well within 5%. Although the gauges are not insulated from the aluminum model, the thermoelectric emf resulting from the material mismatch is small. Details of the gauge design and accuracy are given in Ref. 14.

Typical reservoir pressure and computed heat transfer traces (unsmoothed) are shown in Fig. 4. The heat flux $\dot{q}$ is averaged over a constant reservoir pressure window, e.g., 1 ± 0.2 ms in Fig. 4, before being normalized. The corresponding nondimensional Stanton number St is given by

$$St = \frac{\dot{q}(x)}{\rho_e u_e [h_{aw} - h_w]} \tag{1}$$

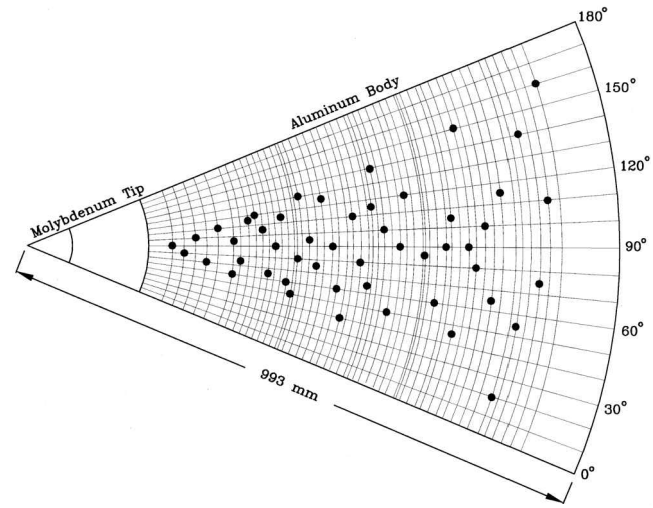

Fig. 3 Developed view of cone model and instrumentation layout.

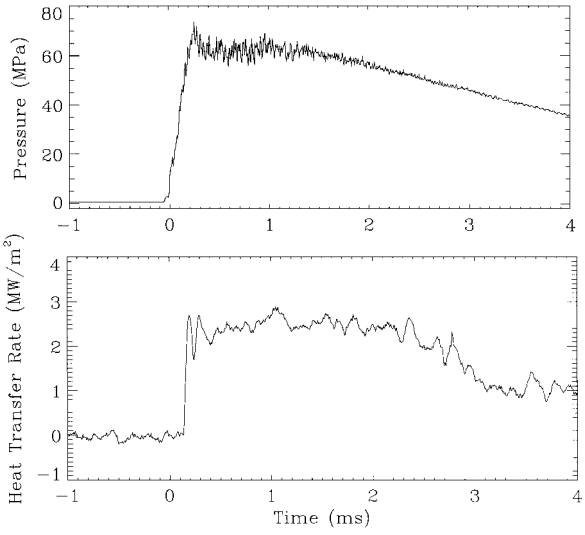

Fig. 4 Typical pressure and heat transfer traces.

where the adiabatic wall enthalpy h_{aw} is given by

$$h_{aw} = h_0 - \tfrac{1}{2}u_e^2(1-r) \tag{2}$$

The boundary-layer-edgeconditions are found by solving the standard Taylor–Maccoll differential equations for conical flow. It is assumed that the chemical composition across the weak conical shock remains frozen. The axial distance is normalized into a Reynolds number given by

$$Re(x) = \frac{\rho_e u_e x}{\mu_e} \tag{3}$$

and a reference Reynolds number given by

$$Re^*(x) = \frac{\rho^* u_e x}{\mu^*} \tag{4}$$

where ρ_e and μ_e are the density and viscosity evaluated at the boundary-layer edge, whereas ρ^* and μ^* are the density and viscosity corresponding to the Eckert reference temperature conditions.[15] Reference conditions are used as conditions more representative of the inner state of the boundary layer than the edge. Heat flux level is used as the primary measure of whether the boundary layer is laminar, transitional, or turbulent.

Scope of Tests and Results

Air and Nitrogen Runs

Over 100 shots were carried out in air and nitrogen. Reservoir pressures were varied from 10 to 85 MPa, and reservoir enthalpies from 4 to 27 MJ/kg. At reservoir enthalpies below 15 MJ/kg, transition could always be observed on the model by tailoring the pressure levels. Above 15 MJ/kg, the Reynolds numbers achieved were too low to promote transition.

Some key enthalpies of reaction involved in these flows are O_2 dissociation at 15.6 MJ/kg and N_2 dissociation at 33.7 MJ/kg. For air, high enthalpy therefore refers to conditions above 17 MJ/kg where substantial freestream dissociation is present. Medium enthalpy refers to conditions between 10 and 17 MJ/kg and low enthalpy below 10 MJ/kg. Other important reactions in air are NO production, dissociation, and ionization.[16] Ranges for nitrogen are slightly higher because there is only N_2 dissociation to consider. A more detailed discussion of hypervelocity boundary layers in air and nitrogen can be found in Ref. 12.

Carbon Dioxide Runs

A total of 35 shots were performed in carbon dioxide with reservoir pressures varying from 40 to 95 MPa and reservoir enthalpies from 3 to 10 MJ/kg. Although similar tunnel parameters (initial shock tube pressure, driver gas pressure, and secondary reservoir pressure) were used for both the air/nitrogen tests and the carbon dioxide tests, the range of enthalpies covered in the latter case was lower because the dissociative real-gas effects of interest occur at lower enthalpy in CO_2. The key enthalpy of reaction in this case is CO_2 dissociation into CO and O around 12 MJ/kg. CO dissociation occurs beyond the maximum enthalpy at which transition was observable on the cone model.

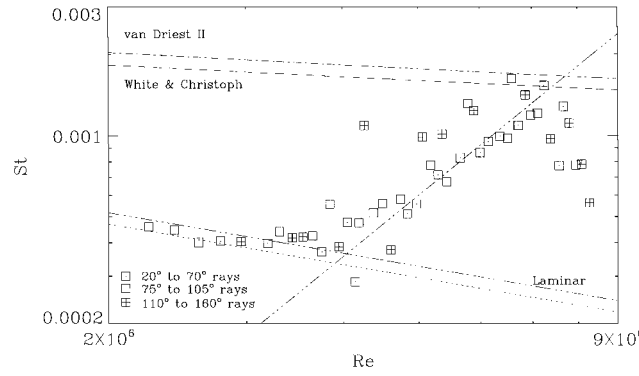

Fig. 5 Typical heat transfer distribution for a transitional boundary layer; shot 1115 (P_0 = 68.7 MPa, h_0 = 7.65 MJ/kg).

Re_{tr}

The state of the boundary layer is determined from the heat flux level measured at the 48 stations along the surface of the cone. Reducing the data to Stanton number vs Reynolds number form, one can then compare the experimental results with established theoretical results for chemically frozen boundary layers.[15]

A typical example is shown in Fig. 5. The dotted line represents the theoretical laminar limit with frozen chemistry. The dashed and the dash–dot lines represent two different turbulence models, also with frozen chemistry.[15] The two other lines are fits of laminar and transitional experimental data. The point of intersection yields the Reynolds number at the beginning of transition. The uncertainty in Re_{tr} is on the order of $\pm 20\%$ and mostly due to the scatter of the laminar data points. The slope of the laminar fit is forced to follow the $Re^{-1/2}$ behavior of a zero-pressure gradient boundary layer. Note that the slight offset of the laminar fit from the theoretical line is probably because the chemistry inside the boundary layer is actually in nonequilibrium.

Measurements on the cone are separated into three azimuthally separated regions to bring out possible flow asymmetries over different sections of the cone. However, rotating the model and the instruments was not found to affect the results.[3] The dropoff at the end is thought to be due to a wave emanating from the nozzle end. The wave angle is steeper at higher enthalpies where the corresponding freestream Mach number is lower.

Enthalpy Effects

As had been observed in the previous study in T5,[3,12] plotting the data in the form of Re_{tr} vs h_0 does not reveal any discernible trends. The new carbon dioxide results are plotted in Fig. 6 alongside the old air and nitrogen data from Fig. 1. The only distinguishing feature is that the CO_2 data lie slightly above the other points. The open symbols in Fig. 6 correspond to cases where the flow was almost completely laminar with a hint of transition. Note that the newer air data, obtained as part of the present study on the more densely instrumented model, do not differ from the old data and have been omitted from the following figures for the sake of clarity. They are included in the following section where only air was of interest.

The new data, however, do reveal distinct trends separating not only air and nitrogen results but also carbon dioxide results, when the Re_{tr} is evaluated at the reference conditions rather than at the edge (Fig. 7). Reference conditions are more representative of the overall inner state of the boundary layer and depend not only on the edge but also on the wall. The new carbon dioxide results are significantly separated from the air and nitrogen data, indicating a much steeper rise with reservoir enthalpy at low values of h_0 and approaching an approximately constant value of Re^*_{tr} at reservoir enthalpies in the range $7 < h_0 < 11$ MJ/kg.

This separation of the data according to the gas suggests that the range of h_0 over which the change in Re^*_{tr} occurs corresponds to

the range in which the dissociation effects appear most strongly and that saturation occurs beyond this range, as seems to happen in the case of CO_2. These data also appear to be consistent with transition through second-mode instabilities. The second mode is theoretically predicted to be the most unstable one at high Mach numbers.[17] These instabilities are acoustic in nature and should be stabilized within the hot boundary layer. Sound waves are known to be absorbed by chemistry,[18] and nonequilibrium effects in the boundary layer are more pronounced as the enthalpy is increased. The latter point also supports the idea that it is conditions inside the boundary layer that affect the transition process rather than conditions at the edge.

Reservoir Enthalpy Normalization

The next issue that arises is how best to reduce the reservoir enthalpy to a corresponding nondimensional form. Because plots against h_0 separate the data according to the gas type, an enthalpy characterizing the gas would probably be the most suitable. For N_2, an obvious choice would be the enthalpy of reaction associated with N_2 dissociation into atomic N. However, for both air and CO_2, there is more than one reaction characterizing the dissociation process, making it more difficult to select a suitable enthalpy of reaction. Because the fluid properties used to calculate the Reynolds number were evaluated at T^*, another choice is the reference enthalpy h^*. The data, however, did not correlate when Re^*_{tr} was plotted against h^*/h_0. Instead, the data did correlate when the reservoir enthalpy was normalized by h_e, but it is not understood why.

Plots of the edge enthalpy h_e over the reservoir enthalpy range of interest are shown in Figs. 8a, 8b, and 8c for air, nitrogen, and carbon dioxide, respectively. The resulting plot of Re^*_{tr} vs h_e/h_0 is shown in Fig. 9. Again the difference between the air/nitrogen data and the carbon dioxide data is well illustrated, but further results at higher and lower enthalpies need to be obtained to confirm any of these apparent trends and whether the air/N_2 data actually overlap with the CO_2 data.

One might also try to reduce both the Re_{tr} and reservoir enthalpy with the conditions at the maximum temperature point within the boundary layer. Should the data correlate, using T_{max} conditions on both axes would resolve the issue of normalizing the different axes with different conditions, as shown in Fig. 9. However, this requires a complete solution of the entire boundary-layer flow including the correct chemistry in the gas phase and at the wall. Although the first set of reactions is well known, the latter, i.e., catalytic wall effects, is far from certain, especially for carbon dioxide.

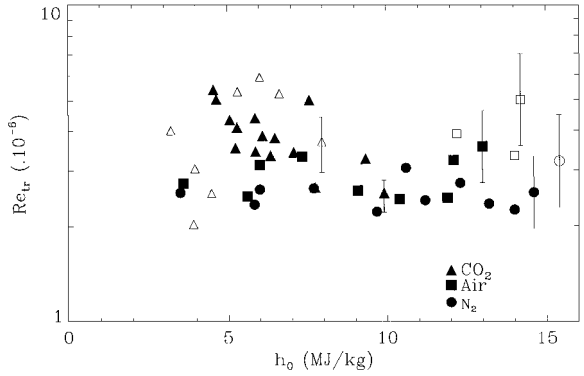

Fig. 6 Re_{tr} **correlation with stagnation enthalpy.**

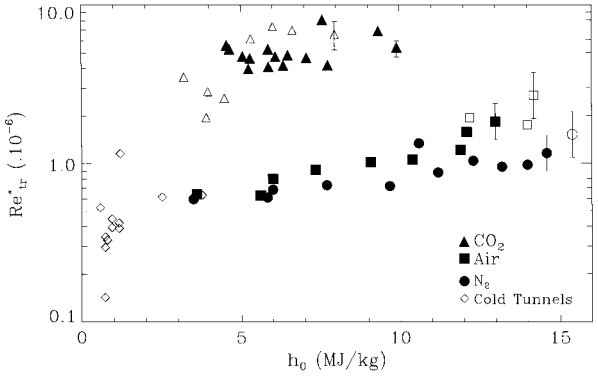

Fig. 7 Re^*_{tr} **correlation with stagnation enthalpy.**

High Enthalpy Free-Flight Data

Free-Flight Re-Entry F Test

A re-entry boundary-layer flight experiment called Re-entry F was declassified in the late 1970s, and a detailed log of both flight

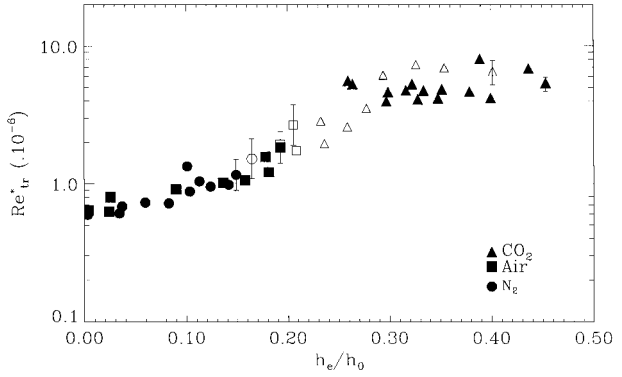

Fig. 9 Re^*_{tr} **vs normalized reservoir enthalpy.**

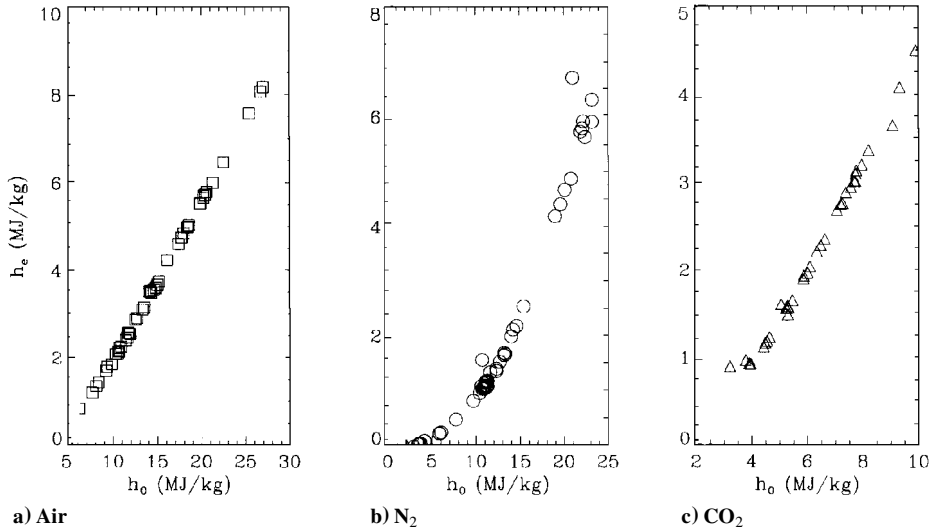

a) Air **b) N_2** **c) CO_2**

Fig. 8 Boundary-layer-edge enthalpy variation with h_0.

conditions and measured Re_{tr} was published by Wright and Zoby.[9] In the free-flight test, a 4-m-long, 5-deg half-angle cone was monitored as it entered the atmosphere from 30.48 to 18.29 km around Mach 20. Pressure and temperature measurements were taken along the surface of the cone, allowing local flow conditions to be deduced. Heat transfer rates were calculated from the temperature traces to determine the state of the boundary layer. Curve fits through the laminar, transitional, and turbulent parts of these heat flux distributions were used to find the beginning and end of transition.

During the measurement period, which lasted approximately 6 s, the freestream Reynolds number varied from 6.56×10^6 to 52.5×10^6 m^{-1} and the corresponding stagnation enthalpy from 18.3 to 16.9 MJ/kg. Figure 10 shows the variation of Re_{tr} with altitude for two different nose recession models used to compute the local flow conditions. The different scenarios also attempted to account for ablation that might have led to an anomaly in the data toward the end of the measurement period. One of the models is a best-case scenario where the tip remains relatively sharp during the period of interest. The other model, ultimately not accepted as possible, is a worst-case scenario with a larger nose radius. The corresponding Re_{tr} vs stagnation enthalpy plot is shown in Fig. 11. Data below 24 km are not included because the ablation results start to differ at that point and measured differential temperatures resulted in bending of the vehicle.

Comparison with Experiment

What makes this test particularly valuable is that the data fall within an enthalpy range attainable by T5, thereby allowing the figures to be directly compared. Furthermore, not only is the geometry of the model used exactly the same as the one in the earlier shock tunnel experiments, but the method of transition detection is also the same.

Figure 12 shows the Re-entry F test Re_{tr} plotted with all of the available T5 air data with respect to stagnation enthalpy h_0. As may be seen, the free-flight results fall more than an order of magnitude above the shock tunnel data. It is sometimes argued that a quiet tunnel would have given closer agreement because of its low disturbance environment.[8]

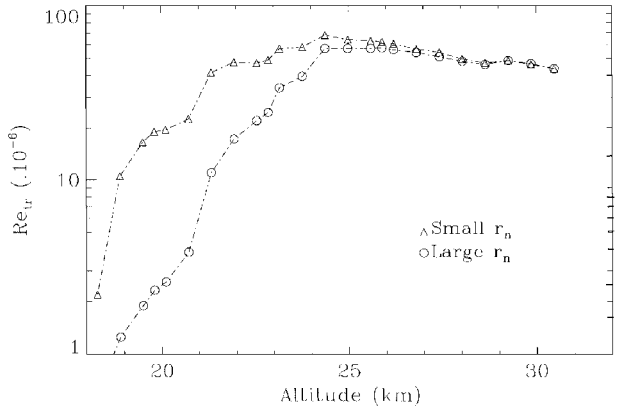

Fig. 10 Altitude variation of Re_{tr} during Re-entry F test.

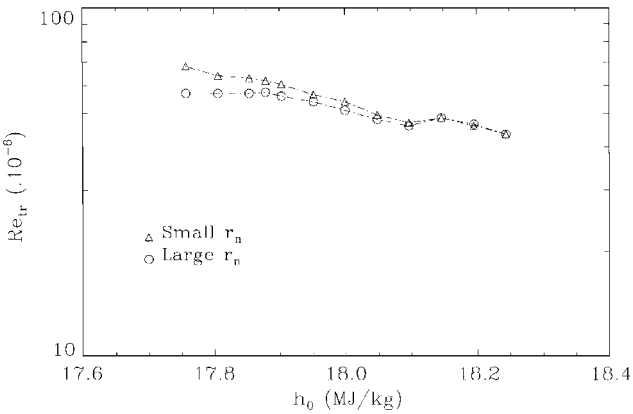

Fig. 11 Stagnation enthalpy variation of Re-entry F test Re_{tr}.

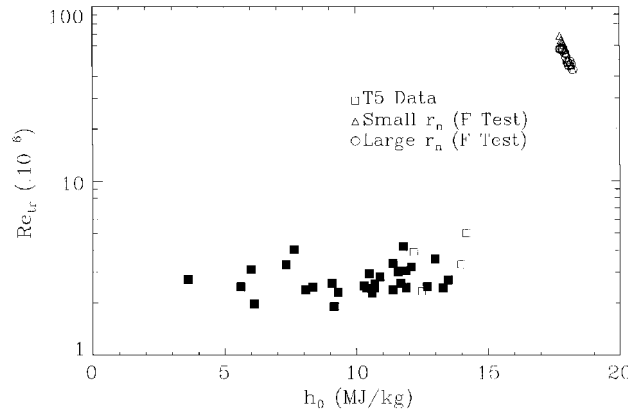

Fig. 12 Free-flight Re_{tr} and T5 air data.

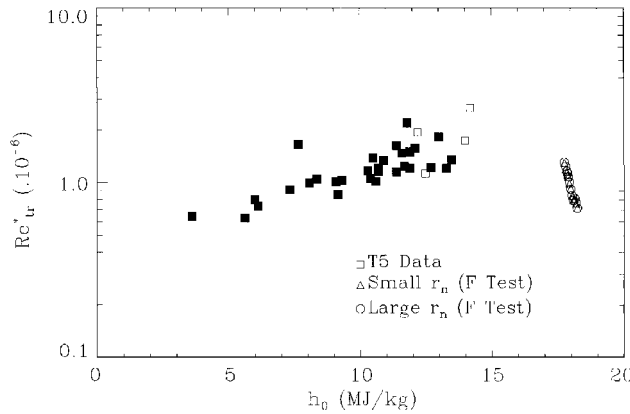

Fig. 13 Free-flight Re^*_{tr} and T5 air data.

When plotting the Re^*_{tr}, however, this distinction disappears and the data collapse to within a very narrow range over the enthalpies considered (Fig. 13). Although the data do not follow the same trend, the experiments show an increase in Re^*_{tr} with increasing enthalpy, whereas the flight figures decrease; there is no longer an order of magnitude of difference between the two. As far as enthalpy effects are concerned, therefore, one appears to be well justified in using reference conditions to represent Re_{tr}. The flight and tunnel freestream conditions for the two flows and, hence, the edge conditions are quite different. However, if the reservoir enthalpies in flight and the tunnel are the same, then the conditions around the maximum temperature points inside the boundary layer itself should be much closer. Reference conditions, more representative of this inner boundary layer state than the edge, are, therefore, preferred.

The different trends in the data can perhaps be explained by the fact that the freestream gas composition is different in the two cases although the velocity is the same. After all, the shock tunnel freestream at high enthalpies is partly dissociated compared to the free-flight environment, which is simply the surrounding atmosphere. Another explanation could be that the flow in free-flight starts out cold in the freestream and heats up to a maximum temperature in the boundary layer before cooling down at the wall. In the tunnel, however, the freestream is already quite hot and the flow does not experience as large a temperature increase to the maximum temperature point inside the boundary layer before reaching the cold wall. The fact that the tip gets progressively blunter, even if it is assumed to be sharp initially, might also contribute to the differences. The nose radius of the cone in the experiments remains relatively constant once it has been through a few runs.

Conclusions

Boundary-layer-transition experiments on a 5-deg half-angle cone at 0-deg angle of attack were presented. The experiments were conducted in the T5 hypervelocity shock tunnel to look for trends

with respect to reservoir enthalpy in three different gases: air, nitrogen, and carbon dioxide.

Results suggest that there is no clear relationship between the Re_{tr}, evaluated at the boundary-layer-edge conditions, and the reservoir enthalpy. Using the reference conditions, however, separates the gases according to how easily they dissociate. For all three gases, the Re^*_{tr} increases with reservoir enthalpy h_0. It also appears that, when the gas reaches a high enough value of h_0 and it is almost fully dissociated, the Re^*_{tr} asymptotes to a constant value. This trend is observed for the case of carbon dioxide; for air and nitrogen, however, one would need to go beyond the current tunnel performance envelope to confirm this. Results at low enthalpies, also out of the reach of current capabilities, might also be useful to understand the lower enthalpy behavior.

Data from free-flight tests, within the T5 enthalpy range, are compared with the current experimental results in air. As expected, the transition freestream Reynolds numbers in free flight are an order of magnitude larger. However, the Re^*_{tr} falls well within the range of the shock tunnel results. The only difference is the opposite behavior with respect to the reservoir enthalpy, but that could be accounted for by the difference in the level of dissociation of the freestream, the fact that the freestream in flight is much colder than in the tunnel, or perhaps a bluntness effect.

Acknowledgments

This work was supported by Air Force Office of Scientific Research University Research Initiative Grant F49620-93-1-0338 (J. Tishkoff). The authors would also like to thank Steven Schneider for bringing the F-test data to their attention.

References

[1]Hornung, H. G., and Bélanger, J., "Role and Techniques of Ground Testing for Simulation of Flows up to Orbital Speed," AIAA Paper 90-1377, June 1990.

[2]Germain, P., Cummings, E., and Hornung, H. G., "Transition on a Sharp Cone at High Enthalpy; New Measurements in the Shock Tunnel T5 at GALCIT," AIAA Paper 93-0343, Jan. 1993.

[3]Germain, P., and Hornung, H. G., "Transition on a Slender Cone in Hypervelocity Flow," *Experiments in Fluids*, Vol. 22, No. 3, 1997, pp. 183–190.

[4]DiCristina, V., "Three-Dimensional Laminar Boundary-Layer Transition on a Sharp 8° Cone at Mach 10," *AIAA Journal*, Vol. 8, No. 5, 1970, pp. 852–856.

[5]Demetriades, A., "Laminar Boundary Layer Stability Measurements at Mach 7 Including Wall Temperature Effects," Air Force Office of Scientific Research, AFOSR-TR-77-1311, Washington, DC, Nov. 1977.

[6]Hornung, H. G., Cummings, E. B., Germain, P., Sanderson, S. R., Sturtevant, B., and Wen, C.-Y., "Recent Results from Hypervelocity Research in T5," AIAA Paper 94-2523, June 1994.

[7]Pate, S. R., "Measurements and Correlations of Transition Reynolds Numbers on Sharp Slender Cones at High Speeds," *AIAA Journal*, Vol. 9, No. 6, 1971, pp. 1082–1090.

[8]Chen, F.-J., Malik, M. R., and Beckwith, I. E., "Boundary-Layer Transition on a Cone and a Flat Plate at Mach 3.5," *AIAA Journal*, Vol. 27, No. 6, 1989, pp. 687–693.

[9]Wright, R. L., and Zoby, E. V., "Flight Boundary Layer Transition Measurements on a Slender Cone at Mach 20," AIAA Paper 77-719, June 1977.

[10]Sudani, N., and Hornung, H. G., "Detection of Driver Gas Contamination in the T5 Hypervelocity Shock Tunnel," AIAA Paper 97-0561, Jan. 1997.

[11]Hornung, H. G., "Performance Data of the New Free-Piston Shock Tunnel at GALCIT," AIAA Paper 92-3943, July 1992.

[12]Germain, P., "The Boundary Layer on a Sharp Cone in High-Enthalpy Flow," Ph.D. Thesis, Graduate Aeronautical Labs., California Inst. of Technology, Pasadena, CA, June 1994.

[13]Schultz, D. L., and Jones, T. V., "Heat Transfer Measurements in Short Duration Facilities," AGARDograph 165, Feb. 1973.

[14]Sanderson, S. R., "Shock Wave Interaction in Hypervelocity Flow," Ph.D. Thesis, Graduate Aeronautical Labs., California Inst. of Technology, Pasadena, CA, May 1995.

[15]White, F. M., *Viscous Fluid Flow*, 2nd ed., McGraw–Hill, New York, 1991, Chap. 7.

[16]Vincenti, W. G., and Kruger, C. H., *Introduction to Physical Gas Dynamics*, Wiley, New York, 1965, Chap. 7.

[17]Mack, L. M., "Boundary-Layer Linear Stability Theory," Special Course on Stability and Transition of Laminar Flow, AGARD Rept. 709, March 1984.

[18]Clarke, J. F., and McChesney, M., *The Dynamics of Real Gases*, Butterworths, London, 1964, Chap. 6.

T. C. Lin
Associate Editor